Construction and Building Materials 253 (2020) 119206

Contents lists available at ScienceDirect

Construction and Building Materials

journal homepage: www.elsevier.com/locate/conbuildmat

Effects of zeolite and silica fume substitution on the microstructure and mechanical properties of mortar at high temperatures

Mehrdad Abdi Moghadam *, Ramezan Ali Izadifard

Department of Civil Engineering, Imam Khomeini International University, Qazvin, Iran

HIGHLIGHTS

- The effects of high temperature on the properties of mortars are clarified.
- The reasons behind the strength gaining at around 400 °C, were justified.
- The order of strength can be estimated by XRD and TGA results.
- The temperature history can be predicted by TGA results.
- The application of zeolite and silica fume meets high temperatures considerations.

ARTICLE INFO

Article history:
Received 30 November 2019
Received in revised form 25 March 2020
Accepted 13 April 2020
Available online 16 April 2020

Keywords:
Mechanical properties
Microstructure
Zeolite
Silica fume
High temperature, temperature history

ABSTRACT

The exposure of concrete to high temperatures leads to mechanical and chemical changes, and the performance of concrete is extremely dependent on its mortar specification. In this study, the compressive and tensile strength of mortar in a temperature range of 28–800 °C is investigated in hot conditions. The microstructure characterization is examined by X-ray diffraction test, thermal gravity analysis, and scanning electronic microscopy test. To minimize the environmental impacts of cement consumption, the possibility of partial replacement of cement with pozzolans is investigated. The results indicate that partial replacement of cement with zeolite and silica fume in the mixing plan of the concrete structure exposed to high-temperature meet both engineering and environmental consideration. Furthermore, the XRD and the TGA results provide valuable information about the prediction of the order of strength and the temperature history of the concrete members. The results pave the way for a better understanding of the high-temperature behavior of pozzolanic mortars.

1. Introduction

Reinforced concrete structures due to ideal thermal properties are suitable for elements exposed to high temperatures. Exposure to high temperatures occurs in the chimneys, the furnaces, the runway of airports, the nuclear reactors, and structures with the risk of fire. Fire accidents could expose reinforced concrete members to high temperatures. The study of concrete properties at high temperatures is carried out in two ways; studying the mechanical properties at the hot condition [1–3] and after cooling [4,5]. The former is for the safety design of the members providing a deep understanding of their real behavior during the fire. However, the latter is to evaluate the behavior of the structures after a fire illustrating its residual strength.

Mortar specifications have a great impact on the overall properties of concrete. Therefore, the importance of investigating and understanding mortar performance at elevated temperatures is of great importance. The strength of concrete is highly attributed to the microstructure of the mortars. Previous studies have shown that increasing temperature, decreases the strength and modulus of elasticity of the mortar [6]. This loss of material strength causes the reduction of the load barring capacity of the elements. However, the selection of suitable materials in the mixing plan can minimize the adverse effects of high temperature [7]. Portland cement is one of the main components of concrete in which the production of cement consumes high energy. High energy consumption produces carbon dioxide that results in global warming and environmental pollution. Previous studies have shown that the contribution of cement production in air pollution is around 7% [8–11]. Therefore, lower cement demand by replacing it with less polluting substances can have a significant impact on the reduction

* Corresponding author.
E-mail address: m.abdimoghadam@edu.ikiu.ac.ir (M. Abdi Moghadam).

https://doi.org/10.1016/j.conbuildmat.2020.119206
0950-0618/

of environmental pollution in the long run [12]. One of the most applicable measures is to reduce cement consumption by replacing it with pozzolans [13,14]. It is worth noting that it is not possible to replace all volumes of cement with pozzolans. According to ASTM 618 standard, pozzolan is silica or alumina-based material that is not self-adhering, but in the presence of moisture and heat reacts with calcium hydroxide, and forms cementitious compounds [15]. Therefore, the optimal percentage of cement replacement with pozzolans is of particular importance. In this regard, Vailpoor et al. tested several dosages of zeolite, silica fume, and metakaolin, concluding that the optimal percentage of cement replacement with mentioned pozzolans is about 10–15%, 7.5–10%, and 10% respectively [16]. The optimal content of zeolite is recommended by 10% and 15% of cement weight by other authors [17–19].

The most significant mechanical properties of mortar are compressive and tensile strength, which have a significant impact on the stability of the concrete structure. Studies have shown that the volume of improvement or loss of strength is extremely dependent on the test type [20]. Therefore, it is important to consider all the mechanical properties of mortars at different temperatures. The tensile strength of mortars has a great impact on the spalling and cracking behavior of concrete. Pore pressure caused by evaporation of water is the most important reason for these damages. Dramatic cracking and even spalling, if the stresses caused by the pore pressure exceed the tensile strength of the mortar, may occur. Therefore, it is important to investigate the tensile strength of mortars at high temperatures [6]. Factors affecting the properties of mortar at elevated temperatures include the rate of rising in temperature, duration of exposure to the target temperature, type of stress, cooling method, and the sample size. Higher mechanical properties are achieved at higher thermal rates and lower exposure duration [21]. The microstructure of cement-based materials is stable up to 400 °C, while exposure to temperatures above 400 °C causes the degradation of hydration products [22]. The size of the specimens results in the difference between the surface temperature and the core temperature of the specimen. This issue causes a thermal gradient between the outer and inner layers of the concrete which causes thermal cracking [23]. The most common cooling methods are water cooling and air cooling. The latter forms micro-cracks by thermal shock on hot specimens resulting in a lower strength [24]. Comparison of compressive and flexural strength loss due to high-temperature exposure showed a higher loss for the flexural strength [22,24]. Various types of pozzolans can be implemented in concrete [13,14,25,26]. The effect of pumice and fly ash on the mechanical properties of normal mortar at temperatures of 300, 600 and 900 °C was investigated by Aydin and Baradan [24]. In this study, the effect of the cooling method on the results was also studied. The results indicated the desirable effect of fly ash incorporation on high-temperature resistance of mortars. Meanwhile, cooling by water resulted in lower strength.

The thermal analysis methods are useful for evaluating the fire behavior of material and present supportive data for interpreting fire test results [27]. Other methods used by researchers to evaluate the microstructure are X-ray diffraction [28] and scanning electron microscopy [29]. The utilization of various percentages of Ground granulated blast furnace slag on the mechanical properties of the pumice mortar and their microstructure was investigated by Aydin. The results showed that the application of Ground granulated blast furnace slag has improved the high-temperature resistance of the mortar significantly [20]. Tanyildizi and Coskun studied the compressive strength of mortar incorporating various contents of silica fume. They reported a declining trend for compressive and tensile strength of the specimens with increasing temperature and found that the optimum dosage of silica fume is 20% of cement weight [30]. Morsy et al. [7] evaluated the performance of mortar containing metakaolin at temperatures up to 800 °C. The experimental results revealed that the compressive and flexural strength of mortars increased up to 250 °C and decreased at higher temperatures significantly. Calcium hydroxide dehydration was reported at temperatures of 500 °C and 600 °C, which is attributed to calcium carbonate decomposition. In this study, the optimal percentage of metakaolin was reported to be 15% of the cement weight. Ibrahim et al. [22] evaluated the compressive strength of high volume fly ash mortar at elevated temperatures. The results showed that the mechanical properties of mortar increased at 400 °C. Using TGA, XRD, and SEM results they further demonstrated that the high-strength mortar could be produced using Nano silica and fly ash. An experimental study conducted by Yazici et al. [6]. They investigated the effect of the high temperatures on the compressive strength of mortars containing fly ash, silica fume, and pumice at various contents. They concluded that pumice-containing mortars had the lowest compressive strength, while the mortars with silica fume had the highest compressive strength at all temperatures. The chemical composition, microstructure, and mechanical properties of high strength mortars containing nano-alumina were examined by Farzadnia et al. [31]. XRD, DSC, and SEM experiments were carried out to identify the chemical constituents and structural changes in the cement matrix after high-temperature exposure. In this study, the results showed that adding overmuch pozzolan to the mortar does not affect the residual compressive strength improvement.

An extensive review of previous studies associated with high temperatures has shown that tests were conducted on cooled specimens. However, a precise understanding of the mortar behavior exposing to high temperatures will obtain by conducting the test on hot specimens. Furthermore, the effect of partial replacement of cement with zeolite or silica fume on the mechanical and microstructure of normal mortar has not been investigated. Therefore, the compressive and tensile strength of specimens in this study are tested at temperatures of 28–800 °C. In this study, the impact of high temperature on the microstructure is clarified by XRD, TGA, and SEM tests. Furthermore, guidelines are proposed for the prediction of the temperature history of the elements that have experienced high temperatures.

2. Experimental program

2.1. Materials

Four types of mortar mixtures were prepared by replacing the cement with zeolite at different mass ratios of 0%(N), 10%(Ze10), and 20%(Ze20). The silica fume replacement ratio was 10% (SF10). The chemical compositions of the cement, zeolite, and silica fume are shown in Table 1. According to this table, the total amount of SiO_2, Al_2O_3, and Fe_2O_3 is 81.06% for zeolite, which meets the chemical requirements according to ASTM C 618–05 [15]. The natural zeolite used in this work was prepared from Semnan in Iran. All batches were prepared using a mechanical mixer confirm-

Table 1
Chemical properties of the cement, natural zeolite, and silica fume.

Chemical composition (% by mass)	Cement	Natural Zeolite	Silica Fume
Silica (SiO_2)	20.24	68.95	93.6
Alumina (Al_2O_3)	5.28	11.14	1.32
Iron oxide (Fe_2O_3)	3.72	0.97	0.37
Calcium oxide (CaO)	63.24	4.83	0.49
Magnesium Oxide (MgO)	2.69	0.79	0.97
Sodium Oxide (Na_2O)	0.258	0.95	0.31
Potassium Oxide (K_2O)	0.533	0.9	1.01
Sulfur Trioxide (SO_3)	2.54	0.068	0.1
Other	1.499	11.402	1.83
Total	100	100	100

ing to the requirements of ASTM C305 [32]. The fine aggregate was river sand having a fineness modulus of 2.8 and a maximum size of 4 mm. Ordinary type 2 Portland cement was used in the mix designs. The characteristics of cement are shown in Table 2.

2.2. Curing and heating regimes

The mixing plan and curing condition for all specimens were constant. The mould was removed 24 h after the specimens were cast. Then, they were cured for 28 days in a water tank. To reduce the risk of spalling during the heating process, the specimens were cured at the laboratory environment for 14 days (Fig. 1). Then, they were heated up at a rate of 1–3 °C/min until the desired temperature was reached (200,300,400,650, and 800 °C). This technique was confirmed by previous researchers [5,31,33]. The heat source was an electric furnace with a capacity of 1200 °C. The specimens were maintained in the furnace for 180 min which makes all parts of the specimens thermally stable and uniform. Tests were performed immediately after transferring them from the furnace. Although a temperature drop occurs after being left the furnace, this temperature loss for the core of the specimens is negligible. To avoid excessive temperature loss, the time of the test after removing the specimens from the furnace should be under 10 min [3].

2.3. Compressive and tensile strength tests

The compressive and tensile strength test of the mortars were measured in accordance with the ASTM C109 [34] and ASTM C 307 [35], respectively. After removing the specimens from the furnace using long clamps, they were tested at the hot state.

2.4. X-ray diffraction test (XRD)

XRD tests were used to evaluate the mineralogical and chemical composition of the specimens. A comparison was made to investigate the changes in the chemical composition of mortars at different temperatures. The required samples were extracted from the inner portion of the specimens and were ground to pass through a 70 μm sieve. The tests were performed through a BRUKER AXS D8 ADVANCE machine using CuK_α source ($CuK_\alpha = 1.5418A^\circ$), 40 kV power and 30 mA. Steps and time per step were 0.025 and 1 s, respectively in the range of 2θ = 4-70°.

2.5. Thermal gravity analysis (TGA)

The TGA tests were used to provide information about the chemical reactions and the portlandite contents of the mortars due to the heating process. A comparison was made for heated specimens exposed to different temperatures. The required samples were extracted from the inner portion of the specimens and were ground to pass through a 70 μm sieve. Tests were conducted using Pyris Diamond TG / DTA thermal analyzer at a heating rate of 10 °C/min under nitrogen atmosphere. In this test, the mass change of a specimen was recorded as the temperature increased from ambient to 900 °C.

Table 2
Characteristics of the cement.

Characteristics		Results
Mineralogical Composition of Clinker	C3S(%)	52.67
	C2S (%)	19.89
	C3A (%)	6.09
	C4AF (%)	11.74
Setting Time (Minutes)	Initial	186
	Final	276
Compressive Strength (MPa)	2Day	16.1
	3Day	23.6
	7Day	31.9
	28Day	50
Physical Properties	Fineness by Blaine Test (cm^2/gr)	3165
	Autoclave Expansion (%)	0.17

Fig. 1. Some of the samples.

2.6. Scanning electronic microscopy test (SEM)

To investigate the changes of the microstructure, formation and decomposing of phases in mortars at elevated temperatures, a Philips XL-30 scanning electron microscope was used. The dimensions of the samples were about 0.5 × 1 × 1 cm and were extracted from the center of each sample. To prevent the repelling of electrons that were emitted by the device, the surfaces of the specimens were coated with a gold alloy film.

3. Results and discussions

3.1. Mechanical properties of the normal mortar at high temperatures

The variation of the compressive and tensile strength of normal mortars with increasing temperature is shown in Fig. 2. The error bar is also shown in this Figure, and the results are the average of three replicates. The overall trend of the compressive and tensile strength curve is almost similar. As the temperature increases, the mechanical properties of the mortar decreases, followed by a significant increase. This increase occurs at 400 °C, where they began to fall sharply. Based on this Figure, the compressive and tensile strength at 400 °C is higher than 300 °C, which can be attributed to the internal curing effects of the mortars at these temperatures. This hypothesis reveals the hydration of un-hydrated particles of the cement under autoclave like curing conditions. The simultaneous presence of pressure and heat in the cement paste layers leads to this condition [36].

3.2. XRD analysis of normal mortar at high temperatures

To explain the effect of high temperature on the mechanical properties of mortars, the results of the XRD test are presented in Fig. 3 and Table 3. Exposure of mortars to high temperatures is accompanied by chemical changes, degradation of microstructure, and ultimately loss of the mechanical properties. The XRD patterns identify phases like Portlandite, Ettringate, C_S_H gel, calcium carbonate, quartz, calcium silicate, and CaO. The mechanical properties of the cement paste are strongly affected by the chemical bonding of the calcium silicate hydrate (C-S-H). Assessment of CSH peaks can help the interpretation of the findings [31,36]. The

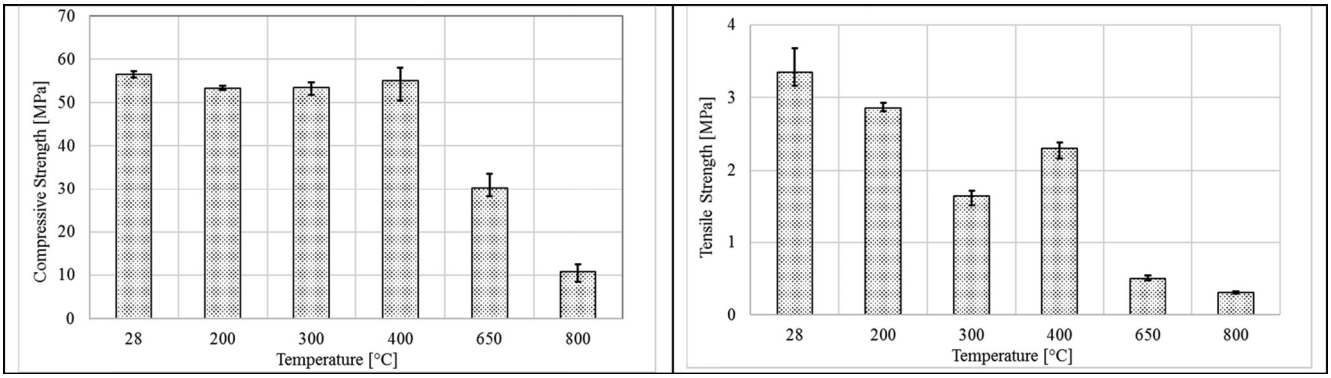

Fig. 2. The Compressive and Tensile strength of normal mortar at temperatures of 28,200,300,400, and 800 °C.

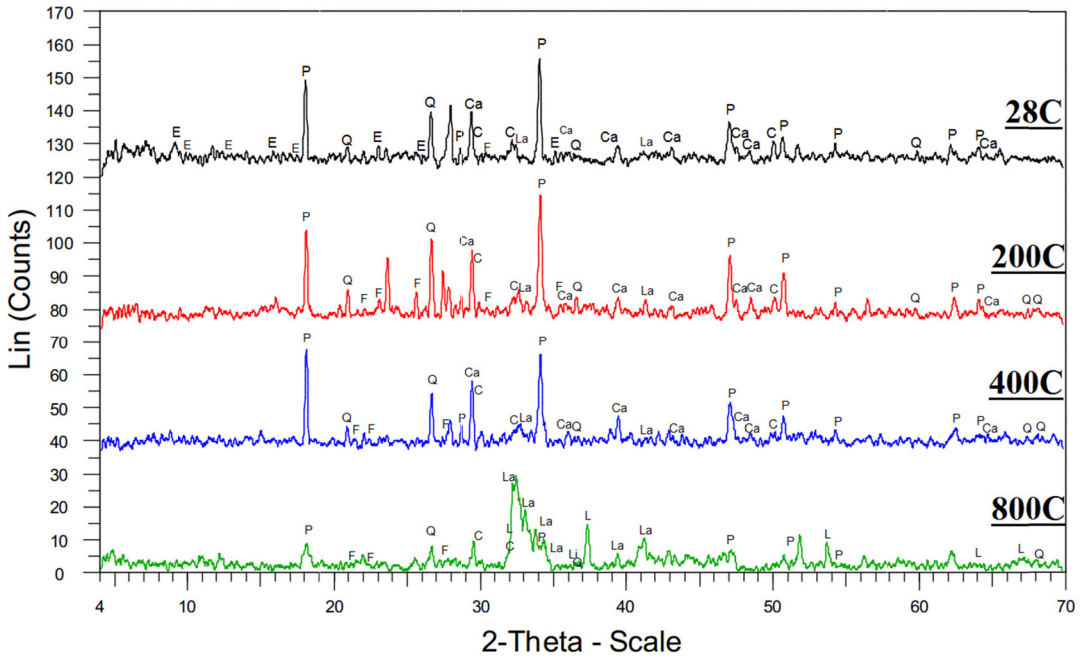

Fig. 3. XRD pattern of the normal mortar at temperatures of 28, 200, 400, and 800 °C (P: $Ca(OH)_2$, C: CSH, E: Ettringite, Q: Quartz, Ca: $CaCO_3$, La: beta-Ca_2SiO_4, and L: CaO).

Table 3
Characteristic of XRD analysis at temperatures of 28–800 °C.

Temperature (°C)	Phase Content (%)						
	Portlandite	Calcium Silicate Hydrate	Ettringite	Calcite	Quartz	beta-Ca2SiO4	lime
28	30.1	9.9	8.8	12.2	7.2	3.7	0
200	23.6	9.5	0	13.9	10	7.1	0
400	35.9	9.2	0	19.8	9.8	6.3	0
800	8	3.2	0	0	3.2	48.9	19.7

quartz peak in the XRD pattern is formed as a result of the broken part of the aggregate components. The intensity of CSH peak at temperatures of 28, 200, 400, and 800 °C are 9.9%, 9.5%, 9.2%, and 6.2%, respectively. These values show that the intensity of CSH peak is almost constant up to 400 °C and has dropped significantly at 800 °C. In terms of ettringite, it is seen that high temperature decomposes this phase, in which ettringite exists only at ambient temperature. The temperature of dehydration and disappearance of ettringite was reported between 80 and 150 °C and 150–170 °C, respectively [37]. Furthermore, Table 3 shows that the chemical changes of microstructure are insignificant at temperatures below 200 °C. Therefore, the loss of compressive and tensile strength of the mortars at these temperatures can be attributed to the evaporation of free water.

Owing to the internal curing condition, which is the reason for strength gaining at temperatures of 400 °C, portlandite is consumed to produce higher content of CSH gels. The XRD patterns at 200 and 400 °C, shows a decrease and an increase of portlandite content, respectively. The increase of portlandite intensity at 400 °C, reveals that the dehydration reaction of portlandite is reversible. Reform of this phase can occur during the cooling duration of the specimens from the mechanical properties test time to the XRD test time. The reversibility of this reaction has also been mentioned in reference [27]. Another reason for the higher amount

of the CH at 400 °C can be justified by the possibility of its partial decomposition. By increasing the temperature from 28 to 400 °C, the intensity of $CaCO_3$ increases from 12.2% to 19.8%. It can be related to the decarburization of portlandite [36]. The increase of this phase can be justified by crack development, which leads to an increase in the permeability. Further increase of temperature to 800 °C indicates an increase of calcium silicate peaks, which is the product of C-S-H decomposition. A comparison of these phases between 28 and 800 °C shows a loss of 40%. However, the calcium silicate peaks increase tenfold. These changes justify a severe decline of strength at temperatures above 400 °C. The peaks of calcium hydroxide fall significantly at 800 °C. The decomposition of calcium hydroxide occurs at a temperature range of 460 °C to 540 °C, which decomposes into CaO and H_2O [37]. Another reason for CaO production is the decomposition of $CaCO_3$ into CaO and CO_2. Past studies have shown that $CaCO_3$ is stable at temperatures below 700 °C, and disappears at temperatures above 700 °C [38]. The intensity of this phase at 800 °C is 19.7%. Another product which is observed at a temperature of 800 °C, is beta-Ca_2SiO_4 (calcium silicate). The emergence of this compound, which has large crystalline particles, can be attributed to the C-S-H decomposition [24,39]. It can be another reason for the sharp decrease in the mechanical properties of the mortar at this temperature. Other observations at 800 °C include a significant decomposition of calcium silicate hydrate peak and portlandite peak.

3.3. TGA analysis of normal mortar at high temperatures

Thermal gravity analysis provides information on the chemical reactions and the portlandite degradation of the mortars due to the heating process. The TGA curve of normal mortar at temperatures of 28–800 °C is presented in Fig. 4. According to this figure, the first weight loss occurs at about 100 °C, which represents the evaporation of free water. Based on this graph, the weight loss at 100 °C is 7.43%. As mentioned in XRD results, ettringite was decomposed at temperatures below 200 °C. Therefore, the weight loss of the sample at this temperature reaches 10.23%. The declining trend in the graph continues to 280 °C. The third major weight loss appeares around 420 °C, and represents the CH decomposition [36]. At this temperature $Ca(OH)_2$ is converted to CaO and H_2O. The forth major weight loss at 630 °C is mainly due to the C-S-H gel decomposition. Another reason for this loss is the decomposition of $CaCO_3$ [40]. The products of this decomposition are CaO and CO_2, in which evaporation of CO_2 results in a higher weight loss. Furthermore, it is seen than the rate of weight loss decreases at temperatures above 650 °C. However, at temperatures above 850 °C, the weight loss remains unchanged.

The TGA results on heated samples are also conducted and are presented in Fig. 4. It is observed that the weight loss due to free water evaporation for the reference sample at 200 °C is 12%. The free water weight loss of heated samples at temperatures of 650 °C and 800 °C, reaches about one percent. In the heated samples, it is observed that the major weight loss occurs at temperatures above the temperature of samples. For example, the weight loss of the N-650 at temperatures below 650 °C was minor. However, a significant weight loss is seen at temperatures above 700 °C. This issue is observed for other samples such as N-300, N-400, N-650, and N-800. In this graph, the final stage of the curves has a zero slope illustrating the decomposition of mortar components. A stable weight of N-800 and N-650 starts from 620 and 725 °C. The start of this stage for specimens exposing lower temperatures is from lower temperatures. This graph can help engineers to predict the temperature history of the members and take the required measures for the rehabilitation of structures after the fire.

The temperature which is linked with the degradation of portlandite is 400 °C for the reference sample [37]. It is believed that specimens that have experienced temperatures of 650 and 800 °C do not experience the weight loss of portlandite occurring at 400 °C. Because these samples have experienced a temperature of 400 °C in the furnace, it is expected that the portlandite must have had decomposed. As this weight loss is seen for N-650 and N-800, it is concluded that the reaction of portlandite decomposition is reversible. Reversibility of this reaction has also been reported by Bakhtiari et al. [27]. This is associated with the recrystallization of the portlandite from curing time at the furnace to TGA test time. Therefore, it can be concluded that the portlandite reforms during the cooling process. This observation confirms the XRD test results. Furthermore, the temperature corresponding to the decomposition of the portlandite for N-650 and N-800 has shifted to about 380 °C. It may be attributed to the decomposition of hydration products and the weakening of the bondings. In contrast, this temperature has shifted further for N-200 and N-400. This can be attributed to the production of higher hydration products and strengthening the bonding of mortar components. These shifts are illustrated in Fig. 4 with vertical lines.

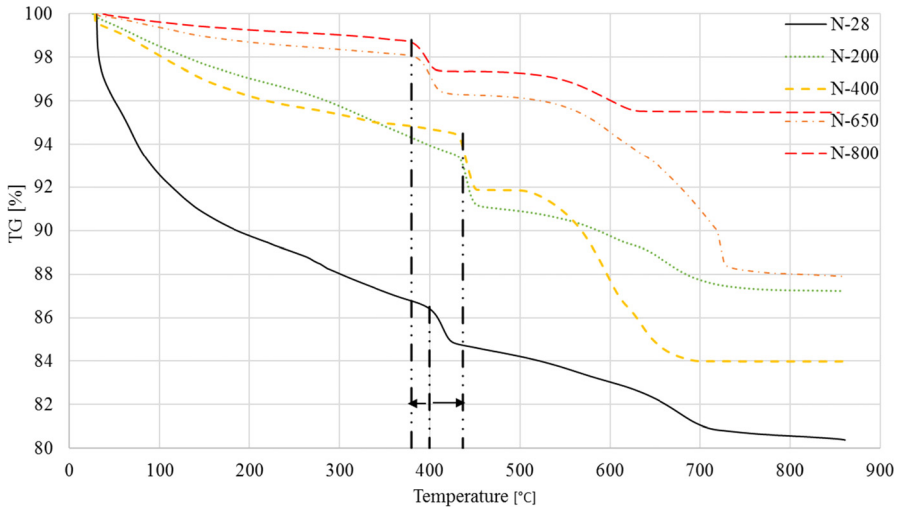

Fig. 4. Comparison of the TGA test results for normal samples at 28, 200, 400, 650 and 800 °C.

3.4. SEM analysis of normal mortar at high temperatures

Fig. 5 presents SEM images with 1250X magnification to illustrate the changes in the microstructure of the normal mortar at temperatures of 28, 200, 400, and 800 °C. Although the microstructure of the mortar is almost porous at ambient temperature, it is denser than higher temperatures. SEM image illustrates CSH gels, large CH crystals, and needle-shaped ettringite components at the ambient temperature. Significant changes in the microstructure of the mortar are observed at temperatures above 200 °C. SEM image at 200 °C, illustrates the disappearances of the ettringite crystals and the establishment of a few voids, resulting from the evaporation of free water. Therefore, the porosity increases and damages durability properties. SEM image of specimens heated up to 400 °C shows that the volume of calcium hydroxide crystals decreases in comparison with the ambient temperature. However, the content of CSH gel increases due to CH consumption. This result confirms the internal curing properties of the mortars at the temperatures between 300 and 400 °C. Another observation in these images is the change in the appearance of CSH crystals with increasing temperature. An increase in temperature has made the CSH crystals thinner and slimmer. This issue causes a decrease in compactness and an increase in density. This deformation is also mentioned in references [7,30]. Therefore, an increase of the sorptivity coefficient, the penetration depth of water, and the electrical resistance of concrete reported in reference [41,42] can be justified.

The micro-cracks have begun to form 400 °C onwards, reaching the highest value at 800 °C. The SEM image of the mortar at this temperature shows severe damages and the expansion of the cracks in terms of number and size. Due to the breakdown of the hydration products, the hair cracks are transformed into a network of connected cracks. These issues separate aggregate from the cement matrix and result in the removal of the aggregate from load-bearing. As seen in Table 3, the content of beta-Ca_2SiO_4 compounds was 48.9% at 800 °C. To observe this composition, five thousand times magnified image of N-800 is shown in Fig. 6. In this figure, rounded fine-grained components might be beta-Ca_2SiO_4. The beta-ca2sio4 compound of this shape was also seen in reference [24].

In order to justify the strength gaining of normal mortar at temperatures of 400 °C, the SEM image of the interfacial transition zone (ITZ) with X100-1250 magnification is shown in Fig. 7.

According to Fig. 2 and the results reported in reference [41–44], it has been observed that the mechanical properties of mortar and concrete increase at about 400 °C. It may be attributed to the inter-layer water evaporation and hardening of the cement paste, which creates a van der Waals force between the cement paste layers. This hypothesis has also been reported in previous references [45]. Fig. 7 shows that the cement paste surrounds the aggregate. Furthermore, the accumulation and expansion of CSH gels are seen.

3.5. The influence of zeolite and silica fume on the mechanical properties of normal mortar

The compressive and tensile strength of normal and pozzolanic mortars at a temperature range of 28–800 °C is presented in Fig. 8. The average coefficient of variation of tested specimens is 5.4%. It is seen from these figures that the overall trend of normal and pozzolanic mortar is similar. The compressive strength at ambient temperature is 56.47 MPa. The replacement of 10 and 20% of cement weight with zeolite decreases the compressive strength by 4.2 and 5.7% to 54.01 and 53.3 MPa, respectively. However, the replacement of 10% of cement weight with silica fume increases the compressive strength by 5.8% to 59.76 MPa. According to this Figure, the replacement of 10 and 20% of cement weight

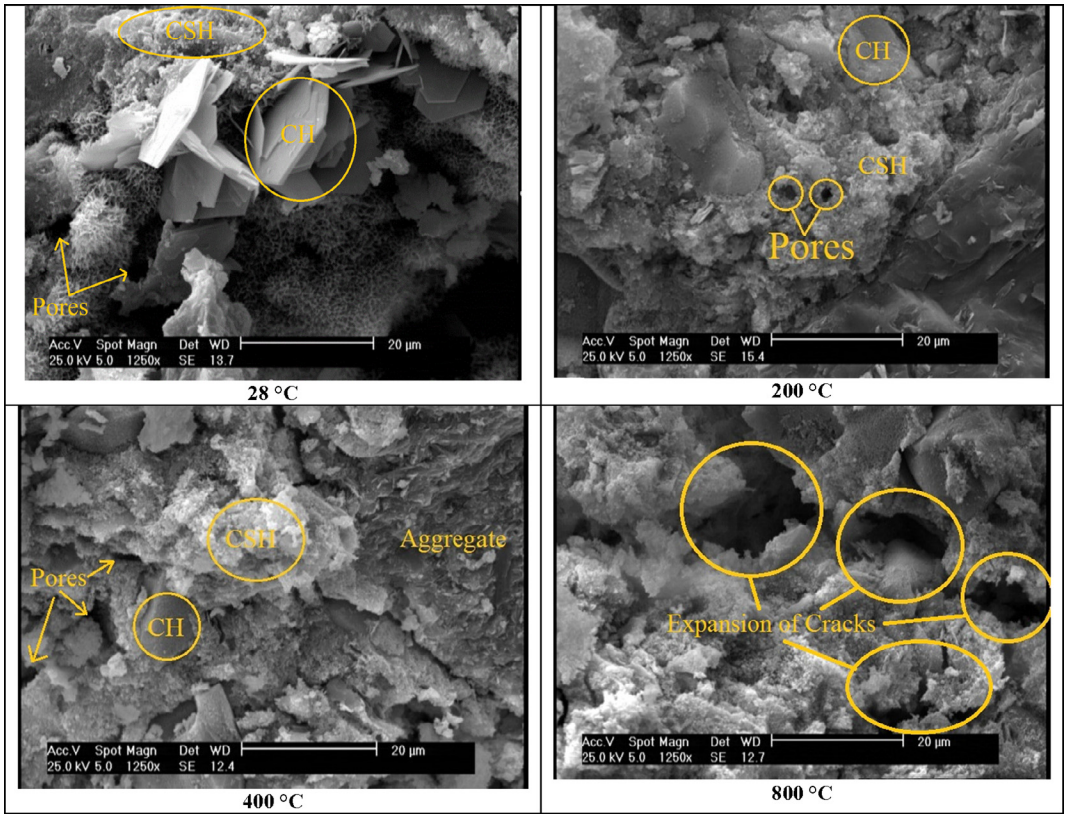

Fig. 5. Deformation of the mortar microstructure due to the exposure to high temperatures.

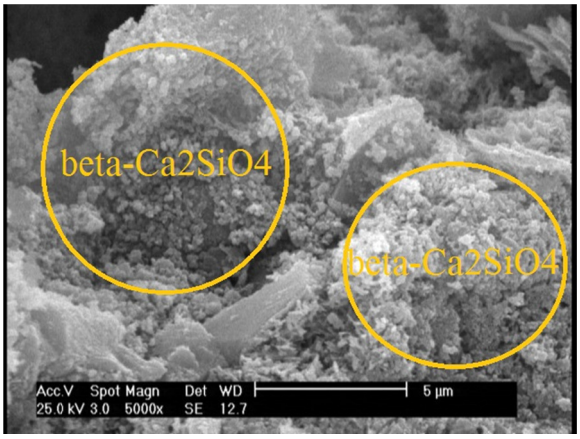

Fig. 6. The presence of beta-Ca2SiO4 compounds at 800° C.

with zeolite reduces the compressive strength of normal mortar by 10.53 and 8.21% on average at the tested temperatures. In contrast, the replacement of 10% of cement weight with silica fume improves the compressive strength of normal mortar by 8.29% on average. The silica fume grains are smaller than the cement grains. Replacement of cement with silica fume fills the voids, consequently increases the density and the compressive strength of normal mortar. Although the particle size of the zeolite similar to silica fume is smaller than the cement grains, owing to the smaller surface area of zeolite in comparison with silica fume, completion of pozzolanic reactions takes more time. This is the reason for a decrease in the compressive strength of the specimens containing zeolite. Because this difference is negligible, especially at temperatures above 400 °C, the application of zeolite is a logical solution for cases with the risk of fire accidents, and elements exposing to high temperatures. It is seen that in specimens containing zeolite, the highest compressive strength before and after 400 °C belongs to Ze10 and Ze20, respectively.

The tensile strength of the normal mortar at the ambient temperature is 3.35 MPa. The substitution of 10 percent of cement weight with zeolite has not changed the tensile strength of normal mortar. However, the higher replacement of zeolite reduces the tensile strength of the mortar by 12.57%. In contrast, a 10% replacement of cement weight with silica fume increases the tensile strength of the mortar by 3.4% to 3.46 MPa. On average, it is observed that the replacement of 10 and 20% of cement weight with zeolite reduces the tensile strength of mortar by 3.45 and 1.46% on average at the tested temperatures. However, a 10% replacement of cement weight with silica fume increases the tensile strength by 27% averagely. Comparison of the tensile strength of Ze10 and Ze20 is similar to the compressive strength results, where the higher tensile strength before and after 400 °C belongs to Ze10 and Ze20, respectively. Higher content of zeolite in mortar increases the possibility of the production of higher hydration products due to the autoclave curing. This issue resulted in a higher tensile strength of Ze20 in comparison with N at the temperatures above 400 °C. According to Fig. 8, it is observed that the tensile strength of normal mortar reduces by 15% at 200 °C. However, previous researches on the tensile strength of concrete at this temperature showed a 70% tensile strength loss [41]. In this study, the reduction of tensile strength was attributed to the

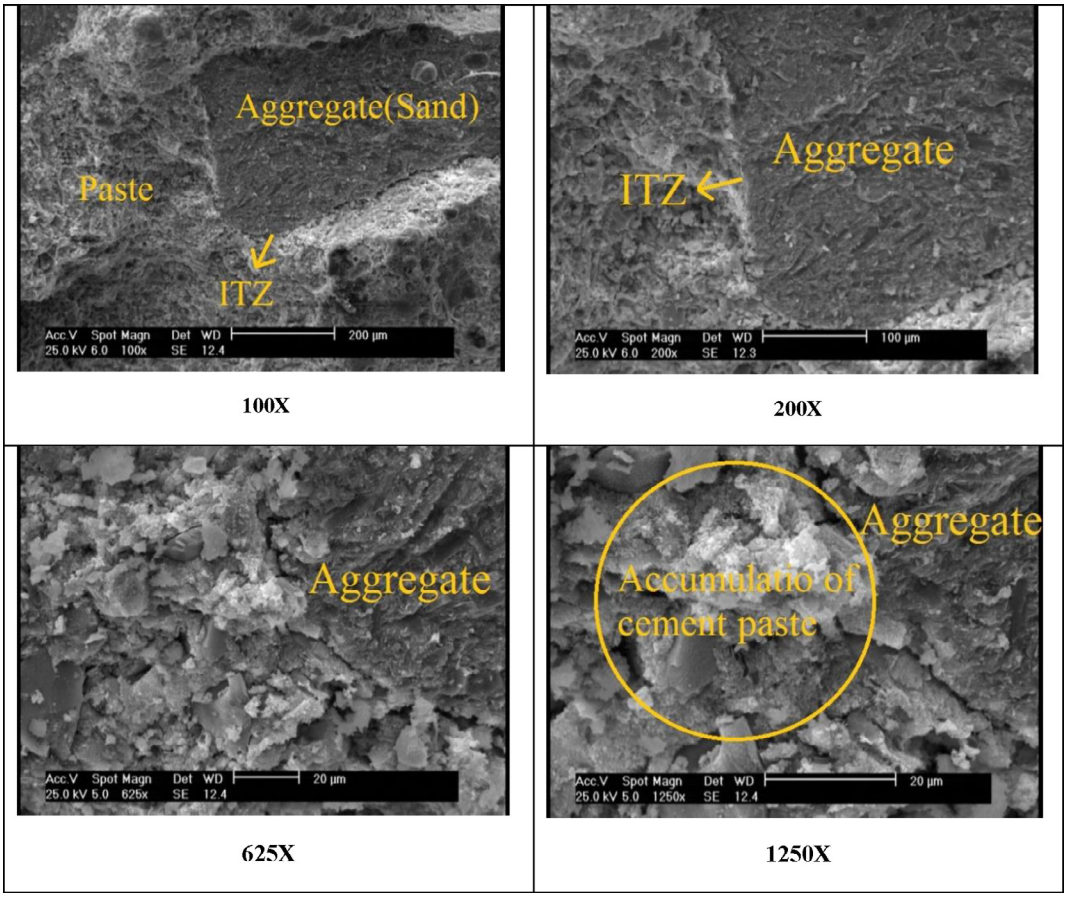

Fig. 7. Hardening of the cement paste at the boundary of the cement matrix and aggregate at 400 °C.

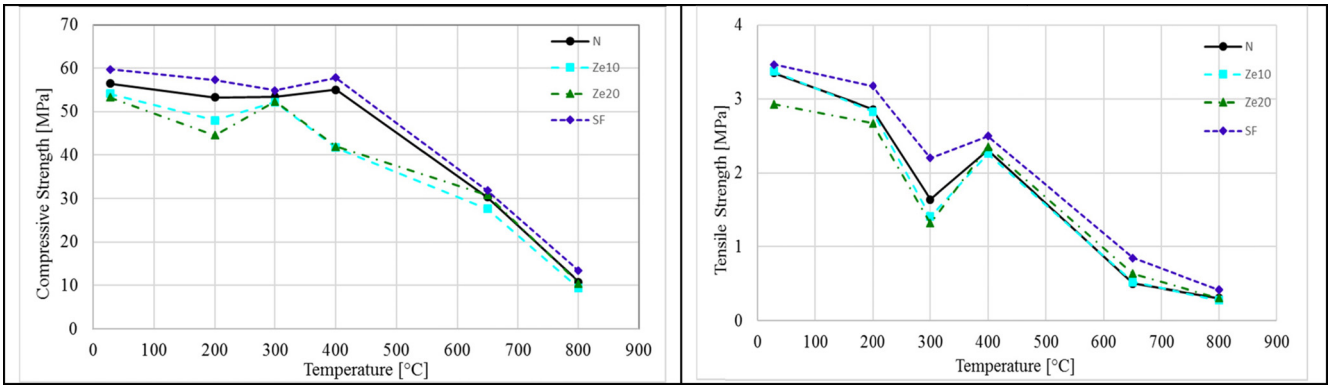

Fig. 8. The compressive and tensile strength of pozzolanic mortars at high temperatures.

simultaneous effect of jack pressure and the outward pressure caused by the evaporation of water. However, in the mortar specimens owing to smaller dimensions in comparison with the cylindrical specimen, the pressure caused by the water vapor is released during the furnace curing. Therefore, the loss of tensile strength resistance is minor in mortar samples. By increasing the test temperature to 200 °C and 300 °C, the compressive and the tensile strength of the mortar decreases, respectively. The XRD results confirm no changes in the chemical composition of mortar at the temperatures below 200 °C. The SEM images illustrated that at these temperatures, the development of hair cracks and voids resulting from the evaporation of free water is responsible for this loss of strength. At this temperature, the compressive strength of N, Ze10, Ze20, and SF are 53.28, 48.02, 44.6, and 57.31 MPa, respectively. It is observed that similar to ambient temperature, the application of zeolite and silica fume decreases and increases the compressive strength of normal mortar, respectively. Based on the responsible factor of strength loss at a temperature of 200 °C, it is expected that the sample with higher permeability will suffer lower damages. The permeability test results reported in reference [6] showed that the order of permeability of the concrete samples was in the form of SF, Ze10, and Ze20, which confirms this forecast. The tensile strengths of N, Ze10, Ze20, and SF at 200 °C were 2.86, 2.83, 2.67, and 3.17 MPa, respectively. As the temperature increases, the mechanical properties of the specimen increase, followed by a sudden drop. This improvement can be justified similar to that described for the normal sample. The mechanical properties of all the samples reduce until they reach their lowest values at 800 °C, attributed to the major changes in the microstructure of the mortar. Another responsible factor for the loss of strength is thermal expansion. The expansion coefficient of mortar is extremely dependent on the constituent particles. The coefficient of thermal expansion of the concrete depends on the moisture content of mortar and the type of the aggregates. This coefficient increases by raising the temperature. Due to the change of the aggregate phase from α to β (at temperatures of 500–600 °C), an increase of the coefficient of the thermal expansion occurs. However, due to the shrinkage of the cement paste the coefficient of thermal expansion of the cement paste decreases at a temperature above 600 °C [46]. The increase in the coefficient of thermal expansion of the cement paste is due to the increase in the volume of free water particles. The loss of this coefficient at higher temperatures is due to the evaporation of water in the C-S-H gel layers [47]. In another study, the results showed that the thermal expansion coefficient of Portland cement paste increased up to 150 °C, followed by a decrease [48]. A significant portion of the concrete is aggregate, and due to high-temperature exposure, they tend to expand. Therefore, the coefficient of thermal expansion of concrete is positive. Changes in the coefficients of the thermal expansion of the components of the mortar results in the expansion of the cracks. This issue is another responsible factor for strength loss at temperatures above 400 °C. Another reason for the loss of the mechanical properties of the samples containing zeolite is related to the reduction of the cement content. Meanwhile, the accumulation of zeolite grains around the cement grains prevents the hydration process of cement, which reduces the hydration products.

3.6. XRD analysis of specimens containing pozzolans at high temperatures

To explain the results of specimens containing zeolite and silica fume, the XRD results are presented in Fig. 9 and Table 4. A comparison of the XRD pattern between mortar containing silica fume and normal mortar shows that the intensity of $Ca(OH)_2$ is lower in the SF specimen. However, the intensity of C-S-H is higher in the SF specimen. The silica fume reacts with the CH and produces additional CSH, which increases the mechanical properties of the normal mortar. In the samples containing zeolite, it is observed that the intensity of $Ca(OH)_2$ is lower than the reference mortar, which indicates the pozzolanic reaction of these samples. The reaction of Al_2O_3 and SiO_2 with $Ca(OH)_2$ is pozzolanic reaction. A comparison of the C-S-H peak intensity among all samples shows that sample containing zeolite has the lowest intensity (Table 4), which justifies the lower mechanical properties of the sample containing zeolite. The XRD graph of the specimen containing zeolite shows 5.4% of zeolite, which also indicates the filler properties of these specimens. This filling effect has a great impact on the improvement of durability properties [41]. The order of the C-S-H peak intensity at 400 °C is also similar to the ambient temperature, i.e. SF, N, and Ze, respectively. The results of the mechanical properties of the samples follow this order. The XRD analysis of the sample containing silica fume at this temperature shows that a part of the CSH phase is converted to the calcium silicate phase(CS), where the intensity of this phase is 9.8%. In other words, it can be stated that the resistance of chemical bonds to the high temperature of C-S-H gels in mixtures containing silica fume is weaker than the reference sample. The examination of the sample containing zeolite shows that the content of portlandite decreases from 17.75 at ambient temperature to 12% at 400 °C. This loss indicates the pozzolanic activity of zeolite.

3.7. TGA analysis of specimens containing pozzolans at high temperatures

The TGA diagrams of all specimens at ambient temperature are illustrated in Fig. 10. It is seen that the residual weight of specimens at the end of the test is 79–82%. Normal and pozzolanic mortar experiences a severe weight loss at temperatures of 400

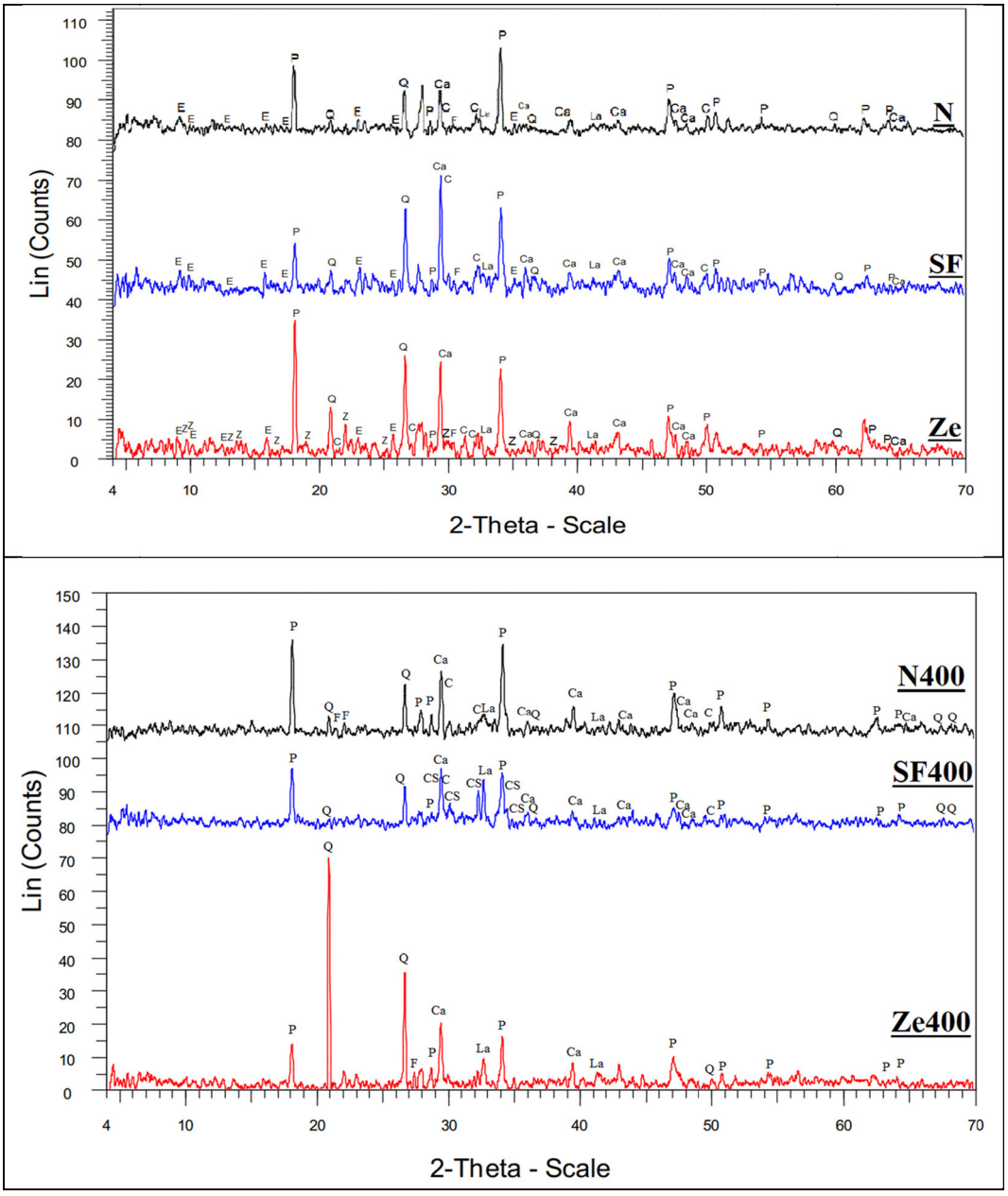

Fig. 9. Comparison of XRD test results for N, SF, and Ze at 28 and 400 °C (C:CSH, P:Ca(OH)$_2$, E:Ettringite, Q:Quartz, Ca:Calcite , Z:Zeolite).

Table 4
Characteristic of XRD analysis of pozzolanic specimens at temperatures of 28–800 °C.

Sample	Temperature (°C)	Phase Content (%)						
		Portlandite	C-S-H	Ettringite	Calcite	Quartz	beta-Ca2SiO4	Zeolite
N	28	30.1	9.9	8.8	12.2	7.2	3.7	0
	400	35.9	9.2	0	19.8	9.8	6.3	0
SF	28	23.4	16.1	10.1	23.1	11.9	8.2	0
	400	24	10.1	0	24.7	10.2	14.6	0
Ze	28	17.7	7.1	7.7	26.9	14.1	7.2	5.4
	400	12	4.9	0	18.4	16.5	6.4	0

and 650 °C. A comparison of TG results shows that the lowest amount of weight loss belongs to the sample containing silica fume. Therefore, silica fume containing mortars have a higher resistance to weight loss. This is attributed to the large quantity of high-density hydration products in SF specimens. A comparison between normal and zeolite-containing samples shows a higher weight loss of zeolite-containing samples at the temperatures below 400 °C. Beyond 400 °C, the weight loss of the zeolite-containing samples is almost similar to normal mortar. However, Ze10 and N experienced similar behavior at temperatures ranges of 400–700 °C. At these temperatures, the TG results of Ze20 are lower than N. Mechanical test results showed that zeolite samples

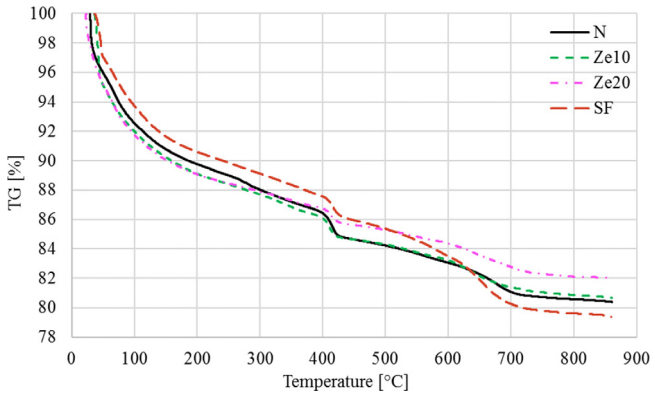

Fig. 10. Comparison of TGA diagrams of the normal and pozzolanic mortars.

had lower mechanical properties than normal mortars at temperatures below 400 °C. However, their mechanical properties were similar to normal mortars at temperatures above 400 °C. A comparison between Ze10 and Ze20 shows that the resistance of Ze10 is higher than that of Ze20 at temperatures below 400 °C. However, this trend was reversed at temperatures above 400 °C. Therefore, it is perceived that using the TGA results, the order of the mechanical properties of mortars can be estimated. Furthermore, the diagram shows a slope of zero at the temperatures above 800 °C, which indicates the destruction of hydration products in pozzolanic samples.

3.8. SEM analysis of specimens containing pozzolans at high temperatures

For a further examination of microstructures, the SEM images of the pozzolanic specimens are also presented in Fig. 11. These images show that normal mortar has a more porous structure in comparison with other specimens, which results in a higher vulnerability of normal concrete durability at ambient and high temperatures. Large amounts of calcium hydroxide are observed in N. Besides, it is observed that numerous pores in the normal sample are filled by the filling effect of these pozzolans. This is the reason for a more effective durability behavior of pozzolanic concrete. The silica fume sample shows a denser microstructure. This is due to the high pozzolanic activity of the silica fume, which was confirmed by XRD results. Therefore, the volume of pores and cracks in comparison with other samples are lower in SF. Comparing the sample containing 10% zeolite with the sample containing 20% zeolite shows a denser structure for the samples containing 20% zeolite. This is due to the existence of more zeolite particles for filling the pores.

4. Conclusions

This study focused on the effects of zeolite and silica fume on the mechanical properties and microstructure of mortar exposed to high temperatures. Based on the results presented in this paper, the following conclusions are drawn:

In this study, the overall trend of mechanical properties of mortars exposed to various temperatures is reported, and the reasons for these changes are discussed. Although it is expected that an increase in the test temperature decreases the mechanical properties continuously, an ascending trend of the mechanical properties is observed at some temperatures. The reason for strength gaining, which occurs at around 400 °C is linked to the internal curing condition, and hardening of the cement paste in the interfacial transition zone. On the other hand, a significant loss of mechanical properties occurs at temperatures above 400 °C, which can be attributed to the degradation of the microstructure component.

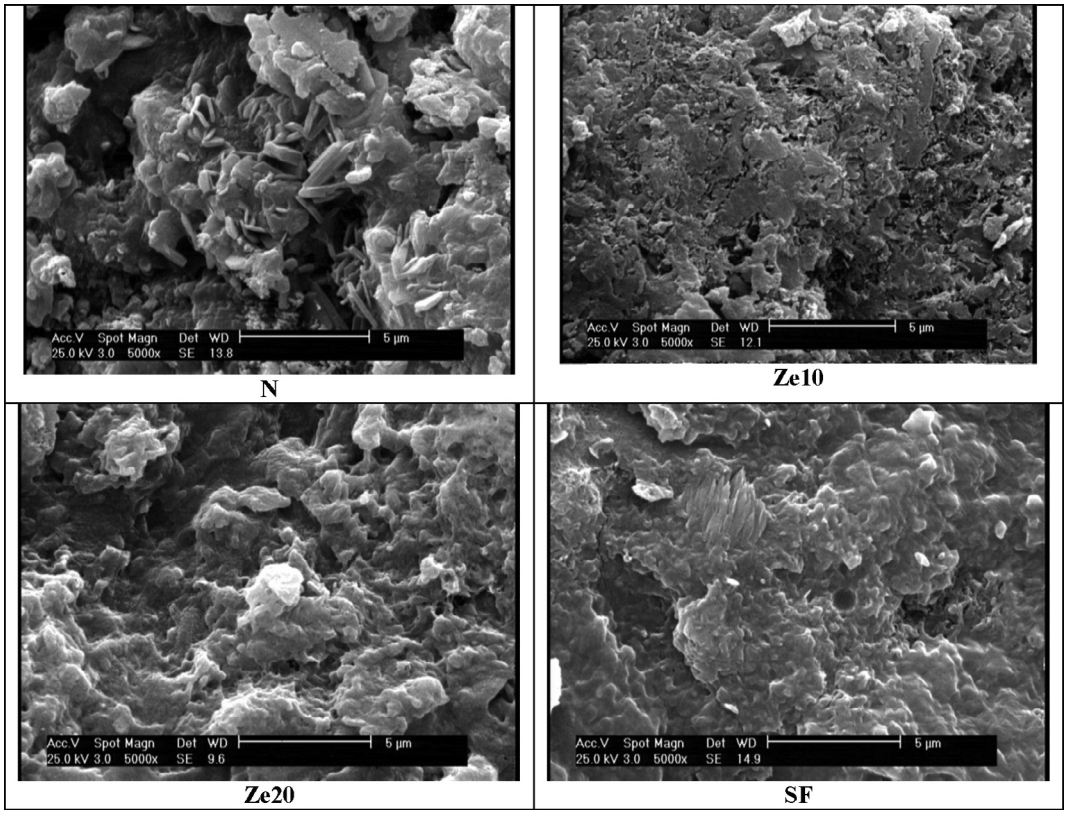

Fig. 11. The effect of pozzolans on normal mortar microstructure.

These observations are confirmed using the XRD, TGA, and SEM tests.

Substitution 10% of cement weight with silica fume can improve the mechanical properties of the normal mortar at all temperatures. On the other hand, the replacement of a portion of cement weight with zeolite slightly reduces the mechanical properties of normal mortar at temperatures below 400 °C; however, it maintained the mechanical properties of mortar at higher temperatures. Comparing various content of zeolite shows that the mechanical properties of Ze20 are lower than Ze10 at temperatures below 400 °C, while this trend is reversed at higher temperatures. Owing to autoclave curing conditions occurring at high temperatures, specimens containing more zeolite enjoy a higher content of secondary hydration products, which results in better mechanical properties. These observations are confirmed using the TGA tests. Specimens with lower weight loss in the TGA test, possess a better mechanical property. This conclusion is generalizable to other specimens, where the lowest amount of weight loss in the TGA test belongs to SF at all tested temperatures. In addition, investigation of the XRD results confirms that the order of the C-S-H peak intensity is consistent with the mechanical results.

A deep investigation on the TGA graph shows a zero slope at the latest stage, illustrating the decomposition of hydration products. For specimens that were exposed to higher temperatures, this stage starts from lower temperatures. Therefore, the topics discussed in the TGA curve can be used for the prediction of the temperature history and order of strength among various mixing plans. These key clues are essential to take the required measures for the rehabilitation of concrete structures.

Finally, it is recommended to use zeolite and silica fume in the mixing plan of concrete structure with the risk of high-temperature exposure to meet both engineering and environmental consideration.

Funding

This research did not receive any specific grant from funding agencies in the public, commercial, or not-for-profit sectors.

CRediT authorship contribution statement

Mehrdad Abdi Moghadam: Methodology, Validation, Investigation, Writing - original draft, Visualization. **Ramezan Ali Izadifard:** Conceptualization, Writing - review & editing, Supervision.

Declaration of Competing Interest

The authors declare that they have no known competing financial interests or personal relationships that could have appeared to influence the work reported in this paper.

Acknowledgments

The authors would like to acknowledge the X-ray laboratory, School of Mining, College of Engineering, University of Tehran, for kind participation and collaborations made throughout the present study. Furthermore, the authors wish to express their thanks to SEM laboratory of Mining and Metallurgical Engineering of the Amirkabir University of Technology, and the concrete laboratory of the Imam Khomeini International University.

Appendix A. Supplementary data

Supplementary data to this article can be found online at https://doi.org/10.1016/j.conbuildmat.2020.119206.

References

[1] P. Bamonte, P.G. Gambarova, A study on the mechanical properties of self-compacting concrete at high temperature and after cooling, Mater. Struct. 45 (2012) 1375–1387.
[2] J. Novak, A. Kohoutkova, Mechanical properties of concrete composites subject to elevated temperature, Fire Saf. J. 95 (2018) 66–76.
[3] J. Novák, A. Kohoutková, Fire response of hybrid fiber reinforced concrete to high temperature, Procedia Eng. 172 (2017) 784–790.
[4] L.W.I. Khalil, Influence of high temperature on steel fiber reinforced concrete, J. Eng. Sustain. Dev. 10 (2018) 139–150.
[5] J. Kim, G.-P. Lee, Evaluation of mechanical properties of steel-fibre-reinforced concrete exposed to high temperatures by double-punch test, Constr. Build. Mater. 79 (2015) 182–191.
[6] Ş. Yazıcı, G.İ. Sezer, H. Şengül, The effect of high temperature on the compressive strength of mortars, Constr. Build. Mater. 35 (2012) 97–100.
[7] M.S. Morsy, Y.A. Al-Salloum, H. Abbas, S.H. Alsayed, Behavior of blended cement mortars containing nano-metakaolin at elevated temperatures, Constr. Build. Mater. 35 (2012) 900–905.
[8] C. Meyer, Concrete materials and sustainable development in the United States, Struct. Eng, Int, 2004.
[9] J.M. Crow, The concrete conundrum, Chem. World. 5 (2008) 62–66.
[10] N. Tošić, S. Marinković, A. Stojanović, Sustainability of the concrete industry: Current trends and future outlook, Tehnika. 72 (2017) 38–44.
[11] J.S. Damtoft, J. Lukasik, D. Herfort, D. Sorrentino, E.M. Gartner, Sustainable development and climate change initiatives, Cem. Concr. Res. 38 (2008) 115–127.
[12] M. Valipour, M. Yekkalar, M. Shekarchi, S. Panahi, Environmental assessment of green concrete containing natural zeolite on the global warming index in marine environments, J. Clean. Prod. 65 (2014) 418–423.
[13] Z. Sun, A. Vollpracht, Isothermal calorimetry and in-situ XRD study of the NaOH activated fly ash, metakaolin and slag, Cem. Concr. Res. 103 (2018) 110–122.
[14] M.C.G. Juenger, R. Snellings, S.A. Bernal, Supplementary cementitious materials: New sources, characterization, and performance insights, Cem. Concr. Res. 122 (2019) 257–273.
[15] C. Astm, 618–05: Specifications for Coal Fly Ash and Raw or Calcined Natural Pozzolan for Use in Concrete, Am. Soc. Test. Mater. (ASTM Int. 100 (2005) 12959–19428.
[16] M. Valipour, F. Pargar, M. Shekarchi, S. Khani, Comparing a natural pozzolan, zeolite, to metakaolin and silica fume in terms of their effect on the durability characteristics of concrete: A laboratory study, Constr. Build. Mater. 41 (2013) 879–888.
[17] T. Markiv, O. Huniak, S. Kh, Optimization of Concrete Composition With Addition of Zeolitic Tuff (2014) 116–120.
[18] K. Samimi, S. Kamali-Bernard, A.A. Maghsoudi, M. Maghsoudi, H. Siad, Influence of pumice and zeolite on compressive strength, transport properties and resistance to chloride penetration of high strength self-compacting concretes, Constr. Build. Mater. 151 (2017) 292–311.
[19] M. Najimi, J. Sobhani, B. Ahmadi, M. Shekarchi, An experimental study on durability properties of concrete containing zeolite as a highly reactive natural pozzolan, Constr. Build. Mater. 35 (2012) 1023–1033, https://doi.org/10.1016/j.conbuildmat.2012.04.038.
[20] S. Aydın, Development of a high-temperature-resistant mortar by using slag and pumice, Fire Saf. J. 43 (2008) 610–617.
[21] A. Benli, M. Karataş, Y. Bakir, An experimental study of different curing regimes on the mechanical properties and sorptivity of self-compacting mortars with fly ash and silica fume, Constr. Build. Mater. 144 (2017) 552–562.
[22] R.K. Ibrahim, R. Hamid, M.R. Taha, Fire resistance of high-volume fly ash mortars with nanosilica addition, Constr. Build. Mater. 36 (2012) 779–786.
[23] D.L.Y. Kong, J.G. Sanjayan, Effect of elevated temperatures on geopolymer paste, mortar and concrete, Cem. Concr. Res. 40 (2010) 334–339.
[24] S. Aydın, B. Baradan, Effect of pumice and fly ash incorporation on high temperature resistance of cement based mortars, Cem. Concr. Res. 37 (2007) 988–995.
[25] L.E. Burris, M.C.G. Juenger, The effect of acid treatment on the reactivity of natural zeolites used as supplementary cementitious materials, Cem. Concr. Res. 79 (2016) 185–193.
[26] M.C.G. Juenger, R. Siddique, Recent advances in understanding the role of supplementary cementitious materials in concrete, Cem. Concr. Res. 78 (2015) 71–80.
[27] S. Bakhtiyari, A. Allahverdi, M. Rais-Ghasemi, B.A. Zarrabi, T. Parhizkar, Self-compacting concrete containing different powders at elevated temperatures–Mechanical properties and changes in the phase composition of the paste, Thermochim. Acta. 514 (2011) 74–81.
[28] R. Dähn, A. Arakcheeva, P. Schaub, P. Pattison, G. Chapuis, D. Grolimund, E. Wieland, A. Leemann, Application of micro X-ray diffraction to investigate the reaction products formed by the alkali–silica reaction in concrete structures, Cem. Concr. Res. 79 (2016) 49–56.
[29] B. Fernandes, A.M. Gil, F.L. Bolina, B.F. Tutikian, Microstructure of concrete subjected to elevated temperatures: physico-chemical changes and analysis techniques, Rev. IBRACON Estruturas e Mater. 10 (2017) 838–863.
[30] H. Tanyildizi, A. Coskun, Performance of lightweight concrete with silica fume after high temperature, Constr. Build. Mater. 22 (2008) 2124–2129.
[31] N. Farzadnia, A.A.A. Ali, R. Demirboga, Characterization of high strength mortars with nano alumina at elevated temperatures, Cem. Concr. Res. 54 (2013) 43–54.

[32] A. Standard, C305, Standard Practice for Mechanical Mixing of Hydraulic Cement Pastes and Mortars of Plastic Consistency, Annu. B. ASTM Stand. (2006).
[33] M.H. Ali, Y.Z. Dinkha, J.H. Haido, Mechanical properties and spalling at elevated temperature of high performance concrete made with reactive and waste inert powders, Eng. Sci. Technol. an Int. J. 20 (2017) 536–541.
[34] C. Astm, 109M–02, Stand. Test Method Compressive Strength Hydraul. Cem. Mortars (Using 2-in. or [50-Mm], Cube Specimens) 109/C (2002).
[35] A. Designation, C307–03 (Reapproved 2012) Standard Test Method for Tensile Strength of Chemical-Resistant Mortar, Grouts, Monolith, Surfacings, 2012.
[36] M.S. Morsy, A.F. Galal, S.A. Abo-El-Enein, Effect of temperature on phase composition and microstructure of artificial pozzolana-cement pastes containing burnt kaolinite clay, Cem. Concr. Res. 28 (1998) 1157–1163.
[37] I. Hager, Behaviour of cement concrete at high temperature, Bull. Polish Acad. Sci. Tech. Sci. 61 (2013) 145–154.
[38] S. Lim, Effects of elevated temperature exposure on cement-based composite materials, (2015).
[39] Q. Zhang, G. Ye, E. Koenders, Investigation of the structure of heated Portland cement paste by using various techniques, Constr. Build. Mater. 38 (2013) 1040–1050.
[40] H. Jang, H. So, S. So, The properties of reactive powder concrete using PP fiber and pozzolanic materials at elevated temperature, J. Build. Eng. 8 (2016) 225–230.
[41] M. Abdi Moghadam, R.A. Izadifard, Experimental investigation on the effect of silica fume and zeolite on mechanical and durability properties of concrete at high temperatures, SN Appl. Sci. 1 (2019) 682. doi:10.1007/s42452-019-0739-2.
[42] M. Abdi Moghadam, R.A. Izadifard, Effects of steel and glass fibers on mechanical and durability properties of concrete exposed to high temperatures, Fire Saf. J. (2020) 102978.
[43] M. Abdi Moghadam, R. Izadifard, Evaluation of shear strength of plain and steel fibrous concrete at high temperatures, Constr. Build. Mater. 215 (2019) 207–216.
[44] R.A. Izadifard, M. Abdi Moghadam, Experimental Study on the shear strength of normal strength concrete at high temperatures, InBook of Abstracts 2019 Aug 20 (p. 44).
[45] C. Castillo, Effect of transient high temperature on high-strength concrete, (1987).
[46] Tayfun Uygunoğlu İlker Bekir Topçu Effect of aggregate type on linear thermal expansion of self-consolidating concrete at elevated temperatures 19 3 2012 10.1515/secm-2012-0015 https://www.degruyter.com/view/j/secm.2012.19.issue-3/secm-2012-0015/secm-2012-0015.xml
[47] Y. Bu, Z. Chang, J. Du, D. Liu, Experimental study on the thermal expansion property and mechanical performance of oil well cement with carbonaceous admixtures, RSC Adv. 7 (2017) 29240–29254.
[48] C.R. Cruz, M. Gillen, Thermal expansion of Portland cement paste, mortar and concrete at high temperatures, Fire Mater. 4 (1980) 66–70.